Energy & Environmental Science

Cite this: DOI: 10.1039/c0ee00640h

www.rsc.org/ees

View Online
Dynamic Article Links

COMMUNICATION

Flexible energy storage devices based on graphene paper†

Hyeokjo Gwon,[a] Hyun-Suk Kim,‡[a] Kye Ung Lee,[a] Dong-Hwa Seo,[a] Yun Chang Park,[b] Yun-Sung Lee,[c] Byung Tae Ahn[a] and Kisuk Kang*[ad]

Received 8th November 2010, Accepted 14th January 2011
DOI: 10.1039/c0ee00640h

Published on 25 February 2011 on http://pubs.rsc.org | doi:10.1039/C0EE00640H
Downloaded on 14 March 2011

Recently, great interest has been aroused in flexible/bendable electronic equipment such as rollup displays and wearable devices. As flexible energy conversion and energy storage units with high energy and power density represent indispensable components of flexible electronics, they should be carefully considered. However, it is a great challenge to fabricate flexible/bendable power sources. This is mainly due to the lack of reliable materials that combine both electronically superior conductivity and mechanical flexibility, which also possess high stability in electrochemical environments. In this work, we report a new approach to flexible energy devices. We suggest the use of a flexible electrode based on free-standing graphene paper, to be applied in lithium rechargeable batteries. This is the first report in which graphene paper is adopted as a key element applied in a flexible lithium rechargeable battery. Moreover graphene paper is a functional material, which does not only act as a conducting agent, but also as a current collector. The unique combination of its outstanding properties such as high mechanical strength, large surface area, and superior electrical conductivity make graphene paper, a promising base material for flexible energy storage devices. In essence, we discover that the graphene based flexible electrode exhibits significantly improved performances in electrochemical properties, such as in energy density and power density. Moreover graphene paper has better life cycle compared to non-flexible conventional electrode architecture. Accordingly, we believe that our findings will contribute to the full realization of flexible lithium rechargeable batteries used in bendable electronic equipments.

[a]*Department of Materials Science and Engineering, KAIST, 291 Daehak-ro, Yuseong-gu, Daejon, 305-701, Republic of Korea. E-mail: matlgen1@kaist.ac.kr; matlgen1@gmail.com; Fax: +82 42 350 3310; Tel: +82 42 350 3381*
[b]*National Nano Fab Center, 291 Daehak-ro, Yuseong-gu, Daejon, 305-806, Republic of Korea*
[c]*Faculty of Applied Chemical Engineering, Chonnam National University, Gwang-ju, 500-757, Republic of Korea*
[d]*Department of Materials Science and Engineering, Seoul National University, Gwanak-gu, Seoul, 151-742, Republic of Korea*
† Electronic supplementary information (ESI) available: See DOI: 10.1039/c0ee00640h
‡ Present Address: Display Laboratory, Samsung Advanced Institute of Technology, Mt. 14-1, Nongseo-Dong, Giheung-Gu, Yongin-si, Gyeonggi-Do 446-712, Republic of Korea

Introduction

Recently, strong interest has been aroused in portable and bendable electronic equipment such as rollup displays and wearable devices.[1] In order to fully achieve functionality of these devices in bendable form, compliant battery units with high energy and power density should be considered.[2–5] However, the fabrication of bendable power sources is a major challenge due to a lack of reliable materials that combine electronically superior conductivity, high mechanical flexibility, and high stability in electrochemical environments. In addition, the cathode and anode, active components of the battery, should also exhibit high electrochemical activity at each desirable potential range.

Broader context

In this paper, we report a flexible electrode based on free-standing graphene paper applied to lithium rechargeable batteries as a new approach to flexible energy devices. Graphene paper is a functional material, which does not only act as a conducting agent, but also as a current collector. The unique combination of its outstanding properties such as high mechanical strength, large surface area, and superior electrical conductivity make graphene paper, a promising base material for flexible energy storage devices. In particular, we find that the graphene based flexible electrode exhibits significantly improved electrochemical performances in almost all aspects of electrochemical properties such as higher energy density, power density and better cycle life, as compared with non-flexible conventional electrode architecture. We believe that the findings of this work will help pave the way for the full realization of flexible lithium rechargeable batteries in bendable electronic equipment. Furthermore, our new approach of using graphene paper as a template for the fabrication of nanostructured electrodes can be applied to various other functional materials, which may be useful in diverse flexible, light weight applications.

View Online

Published on 25 February 2011 on http://pubs.rsc.org | doi:10.1039/C0EE00640H
Downloaded on 14 March 2011

In this work, we demonstrate that freestanding graphene paper can be used as a versatile multi-functional matrix for both the cathode and anode in flexible lithium rechargeable batteries. This is a new approach offering good mechanical flexibility and electrochemical performance of lithium rechargeable batteries.

Carbon based materials are chemically stable within a wide range of electrochemical potentials, and consequently are often used in batteries,[6] supercapacitors,[7] and fuel cells.[8] Among numerous carbon nanostructures, graphene nanosheets (GNS), which are a new class of two-dimensional (2D) carbon nanostructure, have attracted tremendous attention. This is mainly due to their outstanding properties such as high surface area to volume ratio, excellent electronic transport properties, low weight, and high mechanical strength.[9–15] In addition, recent studies have shown that GNS can be easily fabricated in large quantities through chemical conversion from commercially available, inexpensive graphite.[11–14] This manufacturing method enables one to produce macroscopic, paper-like materials of GNS called graphene paper[12] inexpensively. In particular, freestanding graphene paper outperforms many other paper-like materials, such as CNT (carbon nanotubes) paper or graphite foil, in mechanical stiffness and strength.[16,17]

For flexible devices, polymers are typically used as a flexible substrate.[18] However, in light of the fact that commercially cathode materials are fabricated at high temperature, polymers do not offer facile electrode fabrication, since they rapidly degrade at relatively low temperature. Recently developed technologies such as transfer printing of inorganic materials on the polymer require additional complicated processes.[19,20] Also, poor adhesion with oxide materials would be problematic upon long term battery cycling.

As an answer to these problems, we propose a graphene based hybrid electrode as a new approach offering better compatibility and excellent adhesion with the cathode material. Indeed, we found that graphene paper can be a key element functioning both as a current collector and conducting agent. On the basis of these outstanding properties graphene paper, a very reliable material, can be used in diverse flexible forms.

In this work, a graphene-based flexible electrode was applied both to a cathode and anode by employing a pulsed laser deposition (PLD) technique. PLD is a well known technique in fabricating thin-films with its capacity to make high quality oxide ceramics with relatively fast deposition rates. Although it is still hard to deposit in large areas, many engineers are trying to improve the scalability.[21,22] Thus, we expected that PLD technique could be applicable to flexible batteries or other niche markets. We also attempted to integrate these two electrodes in a fully flexible energy device. Interestingly, it was observed that the graphene based flexible cathode exhibits significantly improved electrochemical performance. It can deliver higher energy and power density, a better life cycle when compared to even non-flexible conventional electrode architecture. This is partly ascribed to the close nanoscale contact between GNS and active material at the rugged interface intrinsically presented by GNS.[23–25]

Experimental

Synthesis

Graphene paper was fabricated by filtration of graphene dispersions.[12] In our typical procedure, graphite oxide is synthesized from graphite powder (synthetic, Aldrich) by oxidation with $KMnO_4$, $NaNO_3$, and H_2SO_4 using a modified Hummers method.[26] As-synthesized graphite oxide was dispersed in DI water to make a 0.5 mg ml^{-1} dispersion. The exfoliation of graphite oxide to graphene oxide (GO) was achieved by ultrasonication of the dispersion for 1 h. The obtained suspension was then subjected to centrifugation for 20 min at 3,000 r.p.m to achieve a homogeneous GO dispersion. The pH of the homogeneous GO suspension was adjusted by ammonia solution up to pH 10. A black homogeneous graphene dispersion was obtained by adding hydrazine monohydrate (hydrazine : GO = 1 : 2 in weight) and stirring at 90 °C for 1 h. Graphene paper was made by vacuum filtration of the resulting dispersion through an Anodisc membrane filter (47 mm diameter, 0.2 μm pore size; Whatman), followed by air drying for 24 h at room temperature and peeling from the filter. As-dried graphene paper was then annealed at 550 °C for 2 h under Ar atmosphere for additional deoxygenation. Freestanding graphene paper with a thickness of ~2 μm and a conductivity of ~8 000 S m^{-1} were used for single half-cell making and its integrated flexible system for lithium rechargeable battery.

The cathode material V_2O_5 was grown on graphene paper by pulsed laser deposition (PLD) in a vacuum chamber at a base pressure less than 10^{-5} Torr. The target was prepared by cold pressing from a V_2O_5 powder (99.99%, Kojundo Chem.) and sintering at 600 °C in air for 6 h.[27] A Lambda Physik KrF excimer laser with a wavelength of 248 nm was used in the deposition.[28] The laser fluence and repetition rate were controlled at 2 J cm^{-2} and at 10 Hz, respectively. The thin films were deposited at a room temperature, with an oxygen partial pressure of 20 mTorr. For comparison, cathodic films were also made on an Al foil (Hohsen Corp.) as a conventional current collector.

Characterization

The structures of the graphene paper and V_2O_5 film were investigated by using a D/MAX-RC X-ray diffractometer with Cu-Kα radiation (λ = 1.5406 Å), as well as a high-resolution dispersive Raman microscope (Horiba Jobin Yvon LabRAM HR UV/Vis/NIR), equipped with a charge-coupled device detector. Next, Raman spectra were recorded according to the 514.5 nm line of Ar^+ laser at a power level of 25 mW. The surface morphologies and microstructures were observed by atomic force microscopy (Veeco, Nanoman), scanning electron microscopy (Hitachi S-4800) along with energy dispersive X-ray spectroscopy (EDS), and transmission electron microscopy (FEI, Tecnai F30 S-Twin). EELS analysis is performed with a Cs-corrected STEM (JEM-2100F). The probe size used for EELS analysis was about 1 nm. EELS spectra were analyzed by using Gatan Digital Micrograph software to calibrate the energy scale and remove the background contribution. Electrical conductivity measurements of graphene paper were carried out using a conventional four-point probe method at room temperature. Electrochemical experiments were performed using two-electrode Swagelok-type cells. The graphene paper and V_2O_5/graphene paper were punched in 5/16 inch diameter discs and used in working electrodes directly without an additional current collector. Pure lithium foil (Hohsen Corp.) was used as a counter electrode in lithium rechargeable batteries. For comparison with the electrochemical properties of the graphene paper, conventional graphene electrodes were fabricated by pressing a mixture of graphene powder and PTFE (polytetrafluoroethylene, Aldrich) binder onto Cu or Al foil. A porous membrane (Celgard 2400) is used as a separator. The

 This journal is © The Royal Society of Chemistry 2011

View Online

Published on 25 February 2011 on http://pubs.rsc.org | doi:10.1039/C0EE00640H
Downloaded on 14 March 2011

electrolytes used for lithium rechargeable batteries are 1 M $LiPF_6$ in ethyl carbonate (EC)/dimethyl carbonate (DMC) (1 : 1 by volume, TECHNO SEMICHEM Co., Ltd.). The cells were assembled in an Ar-filled glove box. The discharge and charge measurements were carried out at different current densities on a battery test system (Won-A Tech).

Results and discussion

First, graphene paper as a nanoscale building block (Scheme 1) was tested to fabricate a flexible hybrid cathode for lithium rechargeable batteries. Graphene paper showed the most outstanding properties as a current collector among other carbon based paper electrodes. In the case of CNT paper, electrical features are sensitively affected by the chirality of CNT, which makes the process selective as previously reported.[29] With commercial graphite sheet, both surface roughness and electrical conductivity are inferior to a GNS electrode.

We demonstrate this strategy using V_2O_5 cathode material as a system model. V_2O_5 is known to offer good electrochemical activity as an intercalation host for lithium. Numerous studies have shown its promise as a cathode material, especially in thin film batteries.[30–33] Its amorphous nature combined with low operation voltage is beneficial to the long term cycle life of the cathode,[33] and this is environmentally comparable to that of recently reported amorphous $FePO_4$.[34,35] V_2O_5 can deliver an even higher capacity than $FePO_4$, while the operating voltages of the two materials are comparable at about 3V.

As in previous work,[16] the X-ray diffraction (XRD) pattern of graphene paper (Fig. S1, ESI†) showed a weak and broad (002) peak with a layer-to-layer distance (*d*-spacing) of about 0.349 nm, which is slightly larger than that of pristine graphite (0.336 nm). The increased *d*-spacing of chemically modified graphene paper can be ascribed to the presence of structural defects in some basal planes of GNS, including residual oxygen-containing functional groups.[36] Raman spectroscopy (Fig. S2, ESI†) confirms the formation of GNS with a typically high D/G intensity ratio ($I_D/I_G = 1.15$), compared to that of pristine graphite ($I_D/I_G = 0.21$).[11] A V_2O_5 cathode was grown on the graphene paper through the use of pulsed laser deposition (PLD) at room temperature. The XRD study (Fig. S1, ESI†) indicated the amorphous structure of V_2O_5.

Fig. 1a presents a scanning electron microscopy (SEM) image of typical graphene paper from the top view, showing a rough wavy structure that could originate from the intrinsic wrinkles and ripples of GNS.[23,24] The cross-sectional image, as shown in the inset of Fig. 1a, reveals a compact layer-by-layer stacking of GNS. A plan-view SEM image (Fig. 1b) of V_2O_5 grown on graphene paper exhibits similar nanostructure morphology with high surface area in comparison to that of graphene paper. It suggests that graphene paper serves as a template for the nanostructure of the functional material. In Fig. S3,† atomic force microscopy (AFM) reveals that the surface roughness is around 70–80 nm for both graphene paper and V_2O_5 grown on graphene paper, as compared with below 7 nm for V_2O_5 film grown on a conventional Al current collector. Energy dispersive X-ray spectroscopy (EDS) elemental mappings for V_2O_5 film (Fig. S4, ESI†) reveal uniform distribution of the constituent vanadium and oxygen elements in the film. The cross-sectional transmission electron microscopy (TEM) image (Fig. 1c) shows a V_2O_5 cathode uniformly covering the graphene paper. What is notable is the presence of a heterogeneous region which can be seen from a high-resolution TEM image (Fig. 1d) of the interfaces between the graphene paper and V_2O_5 film. For a more detailed study,

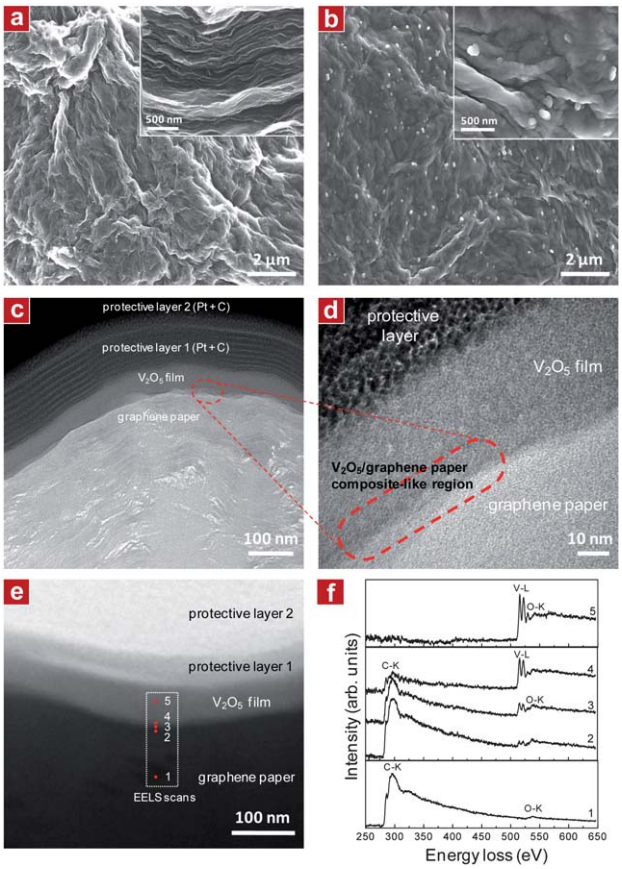

Fig. 1 (a) Plan-view of SEM image of typical graphene paper. The inset shows a cross-sectional SEM image of the graphene paper. (b) Plan-view of SEM image of V_2O_5 film grown on graphene paper. The inset shows a high-resolution SEM image of the sample. (c) A cross-sectional TEM image of V_2O_5 film on graphene paper. To preserve the V_2O_5/graphene paper during the TEM sample preparation, electron beam induced Pt deposition (protective layer 1, Pt particles in carbon matrix) on V_2O_5 film was followed by ion beam induced Pt deposition (protective layer 2, Pt particles in carbon matrix). (d) High-resolution TEM image of the interface between V_2O_5 film and graphene paper. (e) High-angle annular dark-field image for V_2O_5/graphene paper. (f) EELS spectra at various cross-sections of V_2O_5/graphene paper.

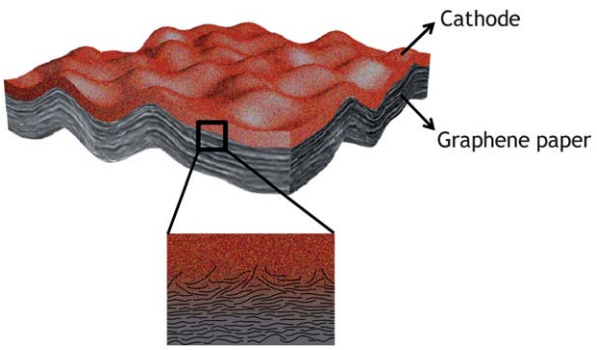

Scheme 1 Schematic representation of the nanostructured functional materials fabricated on flexible graphene paper and the interface of the composite-like structure.

View Online

Published on 25 February 2011 on http://pubs.rsc.org | doi:10.1039/C0EE00640H
Downloaded on 14 March 2011

electron energy loss spectroscopy (EELS) analysis was carried out at various points through the cross-section of the V_2O_5/graphene paper and it confirms the coexistence of two phases, namely V_2O_5 and carbon, in an approximate range of 10 nm near the interface (Fig. 1f). From the EELS analysis, we can indirectly expect that this gradient structure helps enhance the electrical contact at the nanoscale level. The intrinsic wrinkles and ripples on the GNS surface also seem to provide better mechanical and electrical contact through the possible formation of a V_2O_5-GNS composite-like structure at the interface. The issue will be addressed in more detail in the following electrochemical test section.

Galvanostatic charge-discharge tests were used to investigate the lithium insertion/extraction behavior of the nanostructured V_2O_5/graphene paper electrode. Fig. 2a shows the discharge (Li insertion)/charge (Li extraction) curves of the V_2O_5/graphene paper cycled between 3.8 and 1.7 V at a current density of 10 μA cm^{-2}. The corresponding capacities were normalized to the geometrical surface area of the electrode (S = 0.495 cm^2). For comparison, the 2D electrode with V_2O_5 deposited on conventional current collector Al foil under the same deposition conditions was also tested. The charge-discharge profile of both V_2O_5 electrodes showed apparent voltage plateaus, which represents the characteristic of an amorphous V_2O_5 cathode in Fig. 2a.[31] For a more detailed analysis of the charge/discharge mechanism, we obtained dQ/dV data from charge-discharge curves, providing an indirect measure of cyclic voltammetry (CV).[37] In the dQ/dV profiles, shown in the inset of Fig. 2a, broad reduction and oxidation peaks are observed in a range of 1.7–3.8 V.[38] The characteristic broad peaks are attributed to the amorphous nature of V_2O_5, where the Li chemical potential continuously changes with insertion of Li ions. In a separate experiment with graphene alone, where the results are presented in the inset of Fig. 3a, the oxidation and reduction peaks are only observed far below 1 V, implying that graphene does not contribute to the specific capacity in this voltage range of the hybrid cathode.

A reversible volumetric capacity of 4.5 μAh cm^{-2} was observed for the V_2O_5/Al electrode. This result is similar to capacities reported previously for thin film electrodes with amorphous V_2O_5.[31,32] In contrast, a reversible capacity of 21 μAh cm^{-2} was observed for nanostructured V_2O_5/graphene paper, which is more than four times higher than that of the V_2O_5/Al electrode. In addition, the voltage difference between the discharge and charge (*i.e.*, polarization) of the V_2O_5/graphene paper was much lower than that of the V_2O_5/Al electrode. Clearly, the smaller polarization of V_2O_5/graphene paper results in a significantly higher capacity, as shown in Fig. 2a. The smaller polarization of V_2O_5/graphene paper seems to be attributed to its composite-like gradient structure. In general, this heterogeneous structural configuration offers excellent contact at the interface. The intact contact between electrode material and the current collector is important in the electronic transport and reducing undesirable polarization as previous reported in the literature.[25] Fig. 2b also shows that the V_2O_5/graphene paper electrode retains higher capacity at relatively faster rates, from 10 to 600 μA cm^{-2}. The nanostructured V_2O_5/graphene paper still provides 40% of its initial capacity even when the current density increases to 60 times the value, while a conventional V_2O_5/Al electrode retains below 10% of its initial capacity with the same experimental conditions. Comparing with a conventional electrode, we can clearly observe an increase in volumetric capacity at all charge-discharge rates when a nanostructured

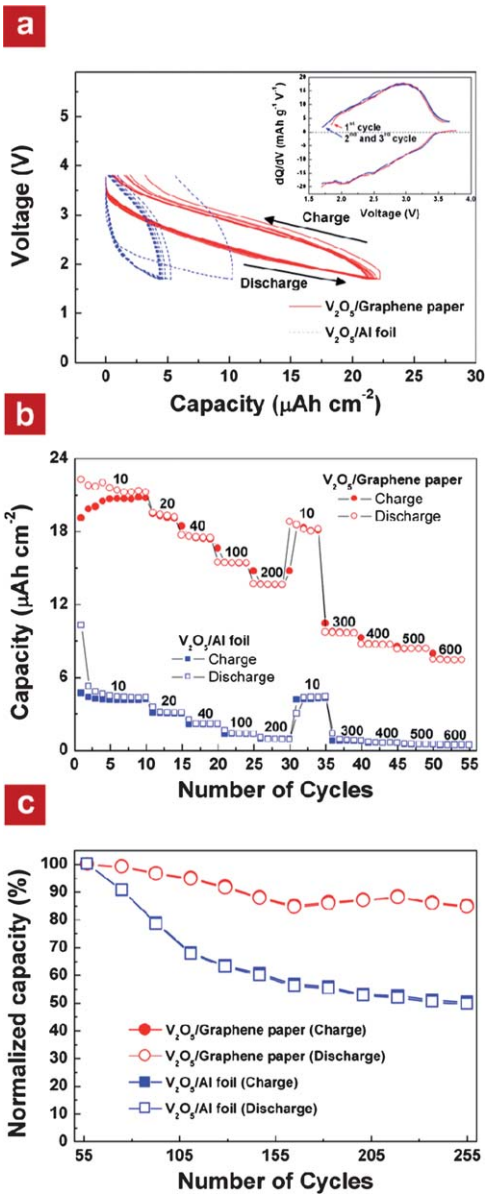

Fig. 2 (a) Charge-discharge profiles for V_2O_5/graphene paper and V_2O_5/Al foil cycled between 3.8 and 1.7 V at a current density of 10 μA cm^{-2}. The dQ/dV profiles are shown in the inset. (b) The volumetric capacity of V_2O_5/graphene paper and V_2O_5/Al foil at various current densities. (c) Cycling performance of V_2O_5/graphene paper and V_2O_5/Al foil up to 200 cycles at a current density of 20 μA cm^{-2} after testing at various current densities shown in Fig. 2b.

graphene hybrid electrode is used. These results suggest that the kinetics of lithium insertion/extraction and electron conduction in V_2O_5/graphene paper is significantly improved. We suppose that this effect can be explained by the gradient structure and rough surface of active materials as shown in AFM RMS analysis of Fig. S4† (*i.e.*, facile charge transport). GNS plays an important role in efficient conduction at the interface of V_2O_5/graphene paper (*i.e.*, composite-like interpenetrating electrode). It was previously reported that the power capability can be significantly improved when a relatively large surface area of electrode is used. This ensures an intact contact between active material and current collector, and graphene paper can stabilize the electrode structure.[15]

 This journal is © The Royal Society of Chemistry 2011

View Online

Published on 25 February 2011 on http://pubs.rsc.org | doi:10.1039/C0EE00640H
Downloaded on 14 March 2011

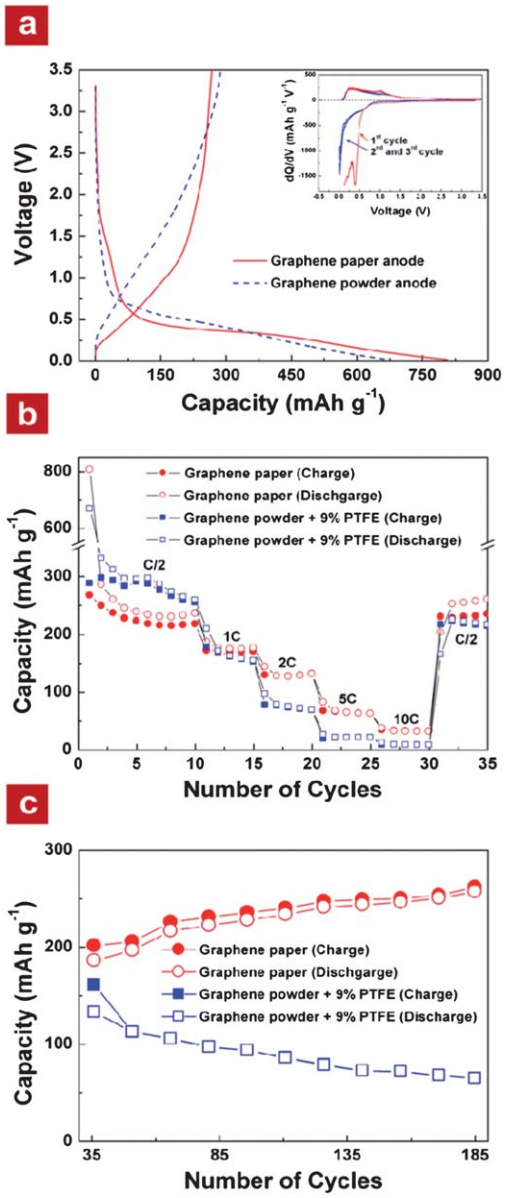

Fig. 3 (a) The first charge-discharge profiles for graphene paper and graphene powder electrode cycled between 0.02 and 3.5 V at C/2 charge/discharge rates. The dQ/dV profiles are shown in the inset. (b) Specific capacity of graphene paper and graphene powder electrodes at different charge/discharge rates. (c) Cycling performance of graphene paper and graphene powder electrodes up to 150 cycles at 1C charge-discharge rates after testing at various rates shown in Fig. 3b.

In addition, as shown in Fig. 2c, we found that the capacity retention of the V_2O_5/graphene paper is superior to that of a conventional electrode on Al foil. Moreover, the fading of the capacity is less than 0.1% per cycle. This is also attributed to the excellent chemical/mechanical robustness of the nanostructure V_2O_5/graphene paper.

Once a flexible graphene/V_2O_5 cathode was successfully fabricated and demonstrated, we attempted to use freestanding bare graphene paper as an anode material in flexible lithium rechargeable batteries. Fig. 3a shows the first charge-discharge profiles of a bare graphene paper anode, cycled between 0.02 and 3.5 V at a rate of C/2. The C-rate is defined as the full use of the material's capacity in one hour, which corresponds to a current density of 371.93 mA g^{-1}. The electrochemical performance of the freestanding graphene paper electrode was compared with the graphene electrode made by pressing a mixture of 95 wt.% grounded graphene powder and 5 wt.% PTFE (polytetrafluoroethylene) binder onto Cu foil as a current collector. The N_2 absorption Brunauer-Emmett-Teller (BET) measurement of the used graphene powder reveals a surface area of 427 m^2 g^{-1} (Fig. S5, ESI†), which is compatible with the reported value.[11] Although the capacity of the graphene paper anode is slightly higher, the charge-discharge curves of both electrodes show similar profiles shapes. In the discharging (Li insertion) curve, large discharge capacities are observed below 0.5 V without distinguishable plateaus. This can be attributed to the disordered GNS stacking.[39] The first discharge capacity of the graphene paper electrode (806.62 mAh g^{-1}) is slightly larger than that of the conventional graphene electrode (669.16 mAh g^{-1}). The large irreversible capacities are observed for both samples reducing to 300 mAh $g^{-1}$and 210 mAh g^{-1}after 5 cycles, respectively (Fig. 3b). This is characteristic of a large irreversible capacity was already previously reported.[36] However, the stabilized capacity at C/2 rate (186 mA g^{-1}) of our sample (300mAh g^{-1}) is significantly higher than the previously reported value (84 mAh g^{-1}measured at slower rate of 50mA g^{-1}).[36] The large irreversible capacity in the first cycle can be explained by the reaction between lithium ions and defects of GNS such as oxygen-containing functional groups. Likewise, the formation of the solid electrolyte interphase (SEI) is partly responsible for the first large irreversible capacity value. In general, the fraction of charge storage due to capacitive contributions increases as electrochemically active materials approach nanoscale dimensions.[40] Therefore, in our experiments, some portion of the capacity can presumably be attributed to the capacitive effect from the nanostructure graphene paper.

The rate capability of both electrodes is investigated and compared in Fig. 3b, where rates up to 10 C are employed. The specific capacity of the graphene paper electrode is slightly larger than that of the conventional graphene electrode at higher rates, suggesting the potential of freestanding graphene paper as an anode material with high-rate capability for flexible lithium rechargeable batteries. The enhanced rate capability of the graphene paper electrode is presumably due to excellent mechanical and electrical reaction between GNS in comparison to that of a conventional graphene electrode. Indeed, the self-standing GNS electrode does not require an additional binder in the electrode fabrication. In contrast, the conventional graphene electrode is obtained by mixing polymer binder (PTFE, 5 wt% of electrode) with graphene powder in order to form the electrode. Since the polymer binder is not as electrically conductive, the total electrical conductivity of the electrode will reduce. Also compared to the random mixing of graphene powder, the aligned layer-by-layer stacking of GNS will promote the electrical contact among graphene necessary for high power performance. Interestingly, the graphene paper electrode showed better capacity retention than the conventional electrode with binder at extended cycles. Fig. 3c shows cycling performances of graphene electrodes at the 1C rate. Graphene paper is able to retain a reversible capacity of more than 200 mAh g^{-1}over 185 cycles, illustrating the excellent mechanical robustness of the freestanding graphene paper. In contrast, the specific capacity of the conventional graphene electrode rapidly decreases to 50% of the initial capacity within 135 cycles. This experiment is consistent with other recent studies of lithium ion storage in GNS powders.[39,41]

View Online

Published on 25 February 2011 on http://pubs.rsc.org | doi:10.1039/C0EE00640H
Downloaded on 14 March 2011

Furthermore, both the cathode and anode maintained the initial morphology even after the cycle test. In the case of the GNS electrode, electrical conductivity also remains at similar values after the cell test. The excellent contact due to gradient structure and compact layer-by-layer structure is attributed to the stable electrochemical cycle behavior.

It is worth noting that the specific capacity of the graphene paper gradually increases as the number of cycles increases. The initial capacity and the capacity after 150 cycles are 201.51 mAh g^{-1} and 261.84 mAh g^{-1} respectively. Our Raman spectroscopy analysis (Fig. S2, ESI†) shows that the intensity ratio ($R = I_D/I_G$) is slightly reduced from 1.15 for the as-fabricated paper to 1.03 for the 150-cycled paper. These values reflect graphitization of graphene paper with the process of lithium ion insertion/extraction. Although deeper research is required to clarify the mechanism, our experiments show that the graphene paper structure can be electrochemically tailored to offer new electrochemical properties, which can be used in diverse applications.

Using the obtained flexible cathode and anode, we demonstrated that the V_2O_5/graphene paper cathode and graphene paper anode can be integrated to build a flexible lithium rechargeable battery (Fig. 4a and 4c). V_2O_5 films of several hundred nanometres were used as a cathode in the complete cell set up. The graphene paper anode was electrochemically lithiated to a potential value of 0.02 V *vs.* Li prior to cell integration since lithium is initially neither present in anode nor cathode. This process eliminates the undesirable lithium uptake in the assembled cell from the first cycle irreversible reaction. Finally, the V_2O_5/graphene paper cathode and the lithiated graphene paper adnode were divided by a separator dipped in liquid electrolyte. The charge-discharge cycles of the assembled battery (Fig. 5) were measured between 3.8 and 1.7 V, at a constant current of 10 μA cm^{-2}. The curve shows the typical charge-discharge behavior of the amorphous V_2O_5 cathode. The first charge and discharge capacity

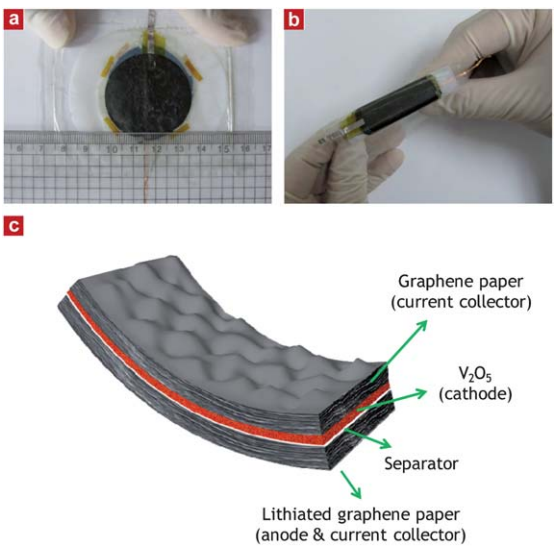

Fig. 4 (a) The assembled flexible Li battery based on graphene paper. V_2O_5/graphene paper and electrochemically lithiated-graphene paper were used as cathode and anode, respectively, which were separated by a separator dipped in liquid electrolyte. (b) The battery is thin, light-weight, and flexible enough to be rolled up or twisted. (c) Schematic drawing of the flexible Li battery based on graphene paper.

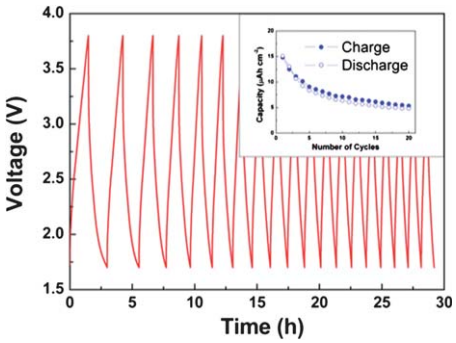

Fig. 5 Charge-discharge curves of the battery device cycled between 3.8 and 1.7 V at a constant current of 10 μA cm^{-2} (inset: capacity *vs.* number of cycles).

were ~15 μAh cm^{-2}, with the negligible first irreversible capacity. (Fig. S6, ESI†) Moreover, during the prolonged cycles, one can successfully observe that charge/discharge of the cell can occur reversibly though it presents a small decrease of capacity. Furthermore, the flexible battery is able to operate when the battery is rolled up or twisted (Fig. 4b) and it shows the charge-discharge capability under full mechanical flexibility. Even though decreased capacity is observed in the full cell, we believe this does not originate from the bending state of the cell, as we observed the same result in the unbended state. Rather, it is due to various engineering factors such as a geometric effect and load balance when two single electrodes are integrated into a full cell in a lab scale fabrication.

Conclusions

In summary, we have demonstrated that a flexible electrode based on freestanding graphene paper can successfully be integrated into flexible storage devices such as lithium rechargeable batteries. The robust integration of graphene into the electrode ensures not only the capability to operate under full mechanical flexibility, but also superior electrochemical performance over conventional electrode architecture. Our finding can suggest further strategy for a full realization of flexible power sources, which can be used in various stretchable/bendable electronic devices. Furthermore, the integration of other functional materials into a nanostructure graphene template could be used in various applications, namely in high-surface area catalysts, photovoltaic devices, and organic light-emitting diodes (OLED). Likewise, we can expect new energy application technology by combining our graphene based, fully flexible lithium rechargeable batteries with other flexible energy generation devices such as bendable solar cells.

Acknowledgements

The first two authors contributed equally to this project. This work was supported by the National Research Foundation of Korea Grant funded by the Korean Government (MEST) (NRF-2009-0094219), a grant from the Fundamental R&D Program for Technology of World Premier Materials funded by the Ministry of Knowledge Economy, Republic of Korea, and Energy Resources Technology R&D program (20092020100040) under the Ministry of Knowledge Economy, Republic of Korea. This research was also supported by the Converging Research Center Program through the

 This journal is © The Royal Society of Chemistry 2011

View Online

Ministry of Education, Science and Technology (No. 2009-0082069, 2010K001088).

Notes and references

1 S. Ju, J. F. Li, J. Liu, P. C. Chen, Y. G. Ha, F. Ishikawa, H. Chang, C. W. Zhou, A. Facchetti, D. B. Janes and T. J. Marks, *Nano Lett.*, 2008, **8**, 997–1004.
2 V. L. Pushparaj, M. M. Shaijumon, A. Kumar, S. Murugesan, L. Ci, R. Vajtai, R. J. Linhardt, O. Nalamasu and P. M. Ajayan, *Proc. Natl. Acad. Sci. U. S. A.*, 2007, **104**, 13574–13577.
3 K. T. Nam, D. W. Kim, P. J. Yoo, C. Y. Chiang, N. Meethong, P. T. Hammond, Y. M. Chiang and A. M. Belcher, *Science*, 2006, **312**, 885–888.
4 H. Nishide and K. Oyaizu, *Science*, 2008, **319**, 737–738.
5 L. Hu, J. W. Choi, Y. Yang, S. Jeong, F. L. Mantia, L.-F. Cui and Y. Cui, *Proc. Natl. Acad. Sci. U. S. A.*, 2009, Online publication.
6 M. Noel and V. Suryanarayanan, *J. Power Sources*, 2002, **111**, 193–209.
7 A. G. Pandolfo and A. F. Hollenkamp, *J. Power Sources*, 2006, **157**, 11–27.
8 A. L. Dicks, *J. Power Sources*, 2006, **156**, 128–141.
9 A. K. Geim and K. S. Novoselov, *Nat. Mater.*, 2007, **6**, 183–191.
10 D. Li and R. B. Kaner, *Science*, 2008, **320**, 1170–1171.
11 S. Stankovich, D. A. Dikin, R. D. Piner, K. A. Kohlhaas, A. Kleinhammes, Y. Jia, Y. Wu, S. T. Nguyen and R. S. Ruoff, *Carbon*, 2007, **45**, 1558–1565.
12 D. Li, M. B. Muller, S. Gilje, R. B. Kaner and G. G. Wallace, *Nat. Nanotechnol.*, 2008, **3**, 101–105.
13 S. Park and R. S. Ruoff, *Nat. Nanotechnol.*, 2009, **4**, 217–224.
14 S. Park, J. An, R. D. Piner, I. Jung, D. Yang, A. Velamakanni, S. T. Nguyen and R. S. Ruoff, *Chem. Mater.*, 2008, **20**, 6592–6594.
15 D. Wang, R. Kou, D. Choi, Z. Yang, Z. Nie, J. Li, L. V. Saraf, D. Hu, J. Zhang, G. L. Graff, J. Liu, M. A. Pope and I. A. Aksay, *ACS Nano*, 4, pp. 1587–1595.
16 H. Chen, M. B. Möller, K. J. Gilmore, G. G. Wallace and D. Li, *Adv. Mater.*, 2008, **20**, 3557–3561.
17 D. A. Dikin, S. Stankovich, E. J. Zimney, R. D. Piner, G. H. B. Dommett, G. Evmenenko, S. T. Nguyen and R. S. Ruoff, *Nature*, 2007, **448**, 457–460.
18 J. Z. Wang, S. L. Chou, J. Chen, S. Y. Chew, G. X. Wang, K. Konstantinov, J. Wu, S. X. Dou and H. K. Liu, *Electrochem. Commun.*, 2008, **10**, 1781–1784.
19 S. I. Park, Y. Xiong, R. H. Kim, P. Elvikis, M. Meitl, D. H. Kim, J. Wu, J. Yoon, Y. Chang-Jae, Z. Liu, Y. Huang, K. C. Hwang, P. Ferreira, L. Xiuling, K. Choquette and J. A. Rogers, *Science*, 2009, **325**, 977–981.
20 D. H. Kim, J. Viventi, J. J. Amsden, J. Xiao, L. Vigeland, Y. S. Kim, J. A. Blanco, B. Panilaitis, E. S. Frechette, D. Contreras, D. L. Kaplan, F. G. Omenetto, Y. Huang, K. C. Hwang, M. R. Zakin, B. Litt and J. A. Rogers, *Nat. Mater.*, 2010, **9**, 511–517.
21 J. M. Lackner, *Surf. Coat. Technol.*, 2005, **200**, 1439–1444.
22 M. Panzner, R. Dietsch, T. Holz, H. Mai and S. Völlmar, *Appl. Surf. Sci.*, 1996, **96–98**, 643–648.
23 J. C. Meyer, A. K. Geim, M. I. Katsnelson, K. S. Novoselov, T. J. Booth and S. Roth, *Nature*, 2007, **446**, 60–63.
24 A. Fasolino, J. H. Los and M. I. Katsnelson, *Nat. Mater.*, 2007, **6**, 858–861.
25 P. L. Taberna, S. Mitra, P. Poizot, P. Simon and J. M. Tarascon, *Nat. Mater.*, 2006, **5**, 567–573.
26 W. S. Hummers Jr and R. E. Offeman, *J. Am. Chem. Soc.*, 1958, **80**, 1339.
27 B. Fleutot, H. Martinez, B. Pecquenard, J. B. Ledeuil, A. Levasseur and D. Gonbeau, *J. Power Sources*, 2008, **180**, 836–844.
28 J. M. McGraw, J. D. Perkins, J. G. Zhang, P. Liu, P. A. Parilla, J. Turner, D. L. Schulz, C. J. Curtis and D. S. Ginley, *Solid State Ionics*, 1998, **113–115**, 407–413.
29 R. M. Tromp, A. Afzali, M. Freitag, D. B. Mitzi and Z. Chen, *Nano Lett.*, 2008, **8**, 469–472.
30 J. B. Bates, N. J. Dudney, D. C. Lubben, G. R. Gruzalski, B. S. Kwak, X. Yu and R. A. Zuhr, *J. Power Sources*, 1995, **54**, 58–62.
31 M. Baba, N. Kumagai, H. Kobayashi, O. Nakano and K. Nishidate, *Electrochem. Solid-State Lett.*, 1999, **2**, 320–322.
32 S. H. Lee, P. Liu, C. E. Tracy and D. K. Benson, *Electrochem. Solid-State Lett.*, 1999, **2**, 425–427.
33 F. Coustier, S. Passerini and W. H. Smyrl, *J. Electrochem. Soc.*, 1998, 145.
34 Y. J. Lee, H. Yi, W. J. Kim, K. Kang, D. S. Yun, M. S. Strano, G. Ceder and A. M. Belcher, *Science*, 2009, **324**, 1051–1055.
35 J. Ryu, S.-W. Kim, K. Kang and C. B. Park, *Adv. Mater.*, 2010, **22**, 5537–5541.
36 C. Wang, D. Li, C. O. Too and G. G. Wallace, *Chem. Mater.*, 2009, **21**, 2604–2606.
37 N. Colaneri, M. Kobayashi, A. J. Heeger and F. Wudl, *Synth. Met.*, 1986, **14**, 45–52.
38 Y. Wang, H. Shang, T. Chou and G. Cao, *J. Phys. Chem. B*, 2005, **109**, 11361–11366.
39 E. Yoo, J. Kim, E. Hosono, H. Zhou, T. Kudo and I. Honma, *Nano Lett.*, 2008, **8**, 2277–2282.
40 T. Brezesinski, J. Wang, J. Polleux, B. Dunn and S. H. Tolbert, *J. Am. Chem. Soc.*, 2009, **131**, 1802–1809.
41 D. H. Wang, D. W. Choi, J. Li, Z. G. Yang, Z. M. Nie, R. Kou, D. H. Hu, C. M. Wang, L. V. Saraf, J. G. Zhang, I. A. Aksay and J. Liu, *ACS Nano*, 2009, **3**, 907–914.

Published on 25 February 2011 on http://pubs.rsc.org | doi:10.1039/C0EE00640H
Downloaded on 14 March 2011